Feedforward Floating Power Supply (High-Response-Speed Equalizer Circuit)*

EIICHI FUNASAKA AND HIKARU KONDOU

Victor Company of Japan, Ltd., Tokyo, Japan

A method for drastically reducing nonlinear distortion and transient intermodulation distortion in noninverting unity-gain amplifiers is described. The method uses a floating power supply with feedforward and boot-strap techniques. Several applications are discussed.

0 INTRODUCTION

Noninverting unity-gain amplifiers find use in many applications, such as impedance converters or active filters. Unity-gain operation requires phase compensation of the open-loop gain for stability. The phase compensation generally results in lowered slew rates and increased high-frequency distortion. This disadvantage can be identified in general-purpose monolithic operational amplifiers. For example, a slew rate of 0.5 V/μs is specified for the operational amplifier RC4558 and 13 V/μs for the FET-input operational amplifier TL-071. Relatively large in-phase signals may cause distortion at the amplifier input. With FET-input operational amplifiers the voltage-dependent nonlinearity of C_{rss} increases the nonlinear distortion at the input with a signal source of high impedance.

This paper describes a new method for reducing distortion and discusses some of its applications.

1 UNITY-GAIN AMPLIFIER CHARACTERISTICS

Fig. 1 shows the basic circuit configuration of the noninverting unity-gain amplifier including two amplifying stages, transconductance amplifier A_1 and buffer A_2. Capacitor C_1 provides phase compensation for stability at unity gain. Fig. 2 shows the open-loop frequency response. General-purpose operational amplifiers have the transition frequency f_T located typically between 1 and 10 MHz. Capacitor C_1 also determines

the upper limit of the slew rate. If the maximum output current of A_1 is I_{max}, the maximum slew rate SR_{max} is

$$SR_{max} = \frac{I_{max}}{C_1} . \tag{1}$$

With amplifiers phase compensated to unity gain, C_1 is generally large, resulting in a low slew rate. For operational amplifiers which are compensated internally, no correction can be made externally. Fig. 3 shows the slew rates of operational amplifiers phase compensated to unity gain. Circuits using discrete components have been tried for higher slew rates, but little progress has been made. Unity-gain amplifiers show satisfactory linearity and operational accuracy at frequencies below 1 kHz. Any method which enables the unity-gain amplifier to keep its superior characteristics up to higher frequencies is expected to find a wide range of applications in the field of audio.

2 BASIC CIRCUIT CONFIGURATION AND ANALYSIS

Fig. 4 shows the basic configuration of a circuit that permits high-speed operation and low distortion. A buffer amplifier A_3, characterized by low output impedance but not necessarily high linearity, can be implemented by a configuration as simple as an emitter follower. Compared with Fig. 1, the capacitor C_1 is not grounded, but is connected to the output of A_3, with the following advantages.

1) Since charge–discharge does not occur in C_1 at frequencies below f_T because of the boot strap of A_3, C_1

     0004-7554/82/050324-06$00.75

does not act as a load on A_1, which improves linearity and significantly increases loop response speed.

2) At frequencies above f_T no signal comes from A_1. The equivalent circuit is shown in Fig. 5. The input signal is fed by feedforward operation of A_3 through A_2 to the output. In the high-frequency range the circuit can be considered a nonfeedback amplifier which cascades A_3 and A_2, with the frequency response dependent on A_3 and A_2.
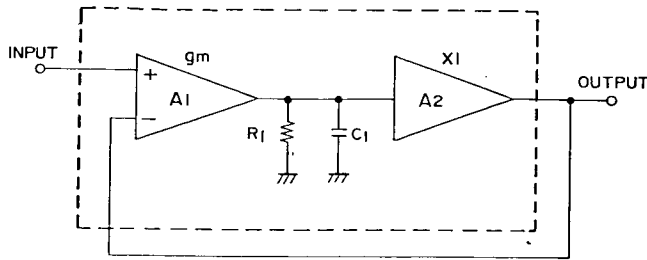

Fig. 1. Basic model of a noninverting unity-gain amplifier.

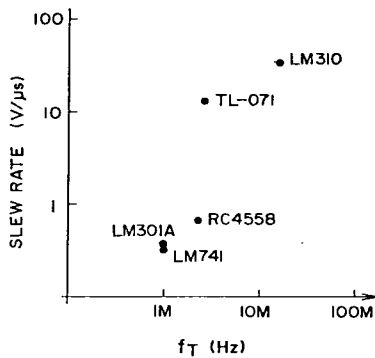Fig. 2. Open-loop gain of an amplifier according to the model of Fig. 1.

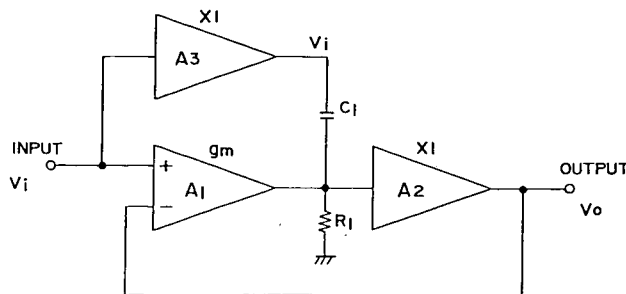Fig. 3. Operational amplifier slew-rate distribution.

Fig. 4. Basic configuration of circuit with high-speed operation and low distortion.

If the cutoff frequencies of A_2 and A_3 are assumed far above f_T for simplicity, the following equations are obtained:

$$(V_i - V_o)g_m \ \frac{R_1}{1 + sT_1} + V_i \ \frac{sT_1}{1 + sT_1} = V_o \qquad (2)$$

with $T_1 = C_1R_1$. Then

$$V_o(1 + g_mR_1 + sT_1) = V_i(g_mR_1 + sT_1)$$

and the transfer function $G(s) = V_o/V_i$ is

$$G(s) = \frac{g_mR_1 + sT_1}{1 + g_mR_1 + sT_1}. \qquad (3)$$

Given $g_mR_1 = 10^4$, for example, Eq. (3) provides a frequency response shown by the solid line in Fig. 6. The high-frequency rolloff reflects the combined effects of the A_2 and A_3 high-frequency rolloffs. If A_3 is omitted, the frequency response is as shown by the broken line in Fig. 6, which corresponds to that shown by the broken line in Fig. 2.

3 CIRCUIT DESCRIPTION

Fig. 7 shows a practical circuit. The heart of the circuit is the feedforward floating power supply (FFPS) enclosed by the dashed line. The circuit provides the same effect as that of Fig. 4 by using an internally phase-compensated operational amplifier whose supply voltage is controlled by the FFPS. As in Fig. 4, the phase-compensation capacitance C_1 is inserted between the input of the output buffer A_2 and the power supply.
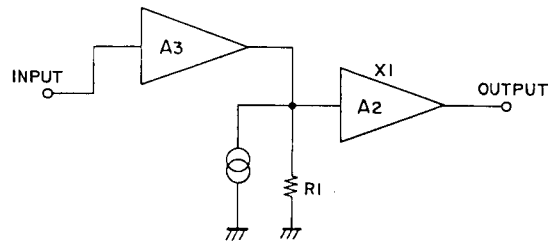

Fig. 5. Equivalent circuit at frequencies above f_T in the circuit of Fig. 4.
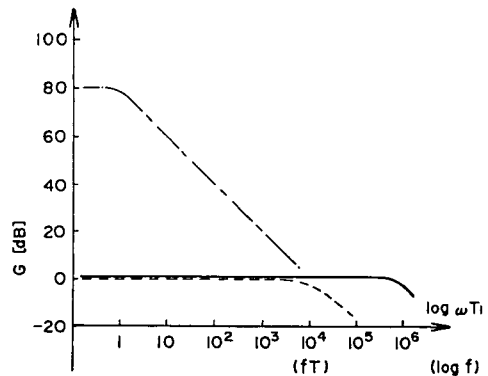

Fig. 6. Frequency response of an amplifier according to the model of Fig. 4.

The FFPS acts as A_3. The configuration has the additional advantage of preventing distortion at the input. With fixed power supplies, any change of input signal voltage may produce a corresponding voltage change between the input and the power-supply rail, resulting in nonlinear distortion at the input. FET-input operational amplifiers are especially conspicuous for distortion at the input. With the FFPS, however, in theory no voltage change of this type occurs, and no input distortion is generated. The supply voltage for the operational amplifier is fixed by the zener diodes D_1 and D_2. The value of $\pm V_{cc}$ can then be chosen according to the output voltage desired, which may be higher than the rated maximum supply voltage for the operational amplifier itself.

4 MEASUREMENT RESULTS

Figs. 8–15 show measurements of the circuit of Fig. 7 using the RC4558 and the TL-071 as operational amplifiers. Comparison of the square-wave responses and the transient intermodulation distortion (TIM) spectral analyses for the RC4558 in Figs. 8–10 shows the advantage of FFPS. Its use increases the slew rate from ± 0.75 V/μs to ± 300 V/μs and reduces TIM to a level that cannot be measured. For TIM measurement a low-pass-filtered ($f_c = 100$ kHz) composite signal of 3.18-kHz square wave and 15-kHz sine wave with an amplitude ratio of 4:1 is used as a test signal. The spectrum of the test signal is the same as that shown in Fig. 10.

Comparison of the total harmonic distortion characteristics for the operational amplifier RC4558 in Figs. 11 and 12 shows a significant reduction in total harmonic distortion and increased maximum output amplitude with FFPS. The improvement is closely corre-

lated with the reduction in TIM described above. Figs. 13–15 show the total harmonic distortion characteristics obtained for the FET-input TL-071. Generally FET-input operational amplifiers cause nonlinear distortion at the input because of the voltage-dependent C_{rss}. Figs. 14 and 15 show that the greater the source impedance, the higher the total harmonic distortion. The FFPS reduces the distortion and keeps it at much lower levels even at high frequencies, as shown in Fig. 13. The slew rate in this case is as high as ± 200 V/μs.

Fig. 11 shows that an output voltage greater than the rated supply voltage of the RC4558 (± 18 V) can be obtained with an FFPS voltage $\pm V_{cc}$ of ± 50 V.

5 APPLICATIONS

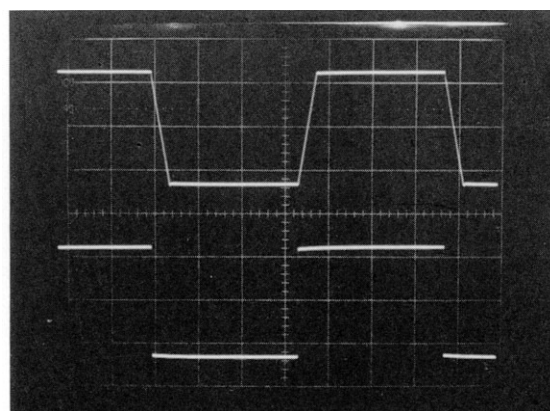The FFPS can be applied to a circuit that operates in

Fig. 8. Square-wave response of practical circuit of Fig. 7 with operational amplifier RC4558. $f = 20$ kHz; vertical scale 2V/div. upper trace—without FFPS, SR $= \pm 0.75$ V/μs; lower trace—with FFPS, SR $= \pm 300$ V/μs.
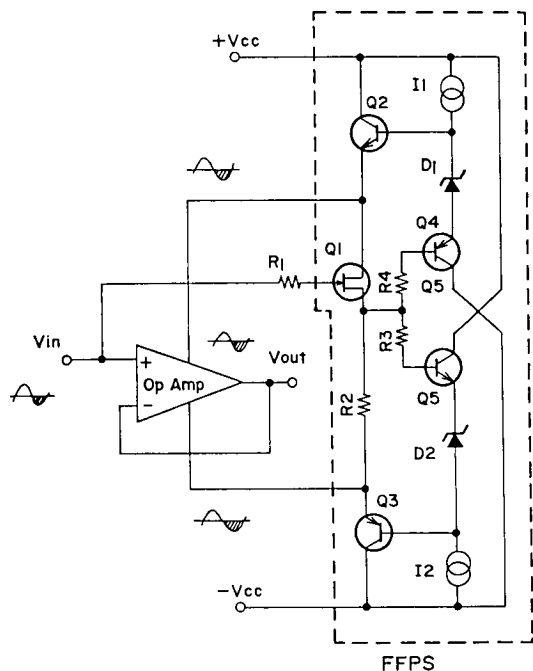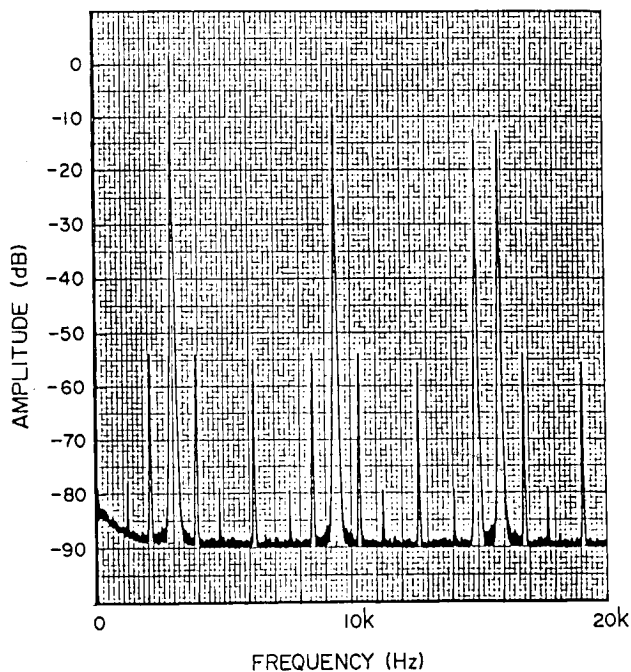

Fig. 7. Practical circuit configuration.

Fig. 9. TIM spectral analysis of practical circuit of Fig. 7 without FFPS, with operational amplifier RC4558.

the noninverting unity-gain mode, whether it is built with monolithic integrated circuits or with discrete components.
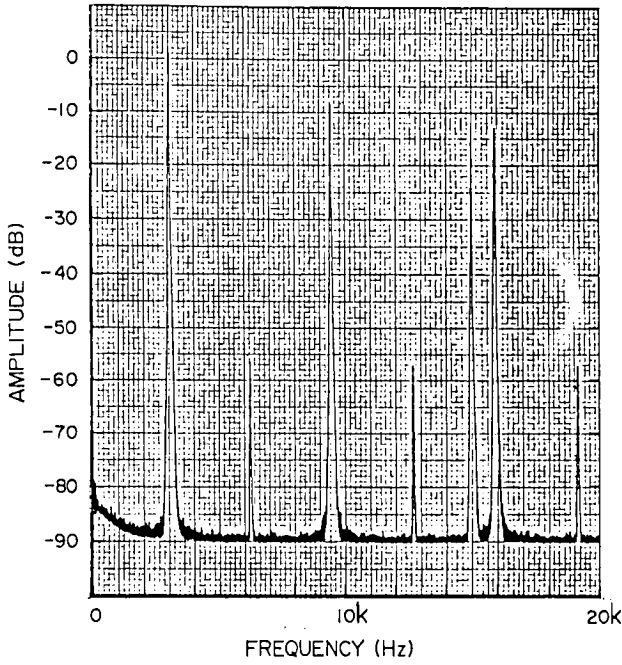

Fig. 10. TIM spectral analysis of practical circuit of Fig. 7 with FFPS, with RC4558.
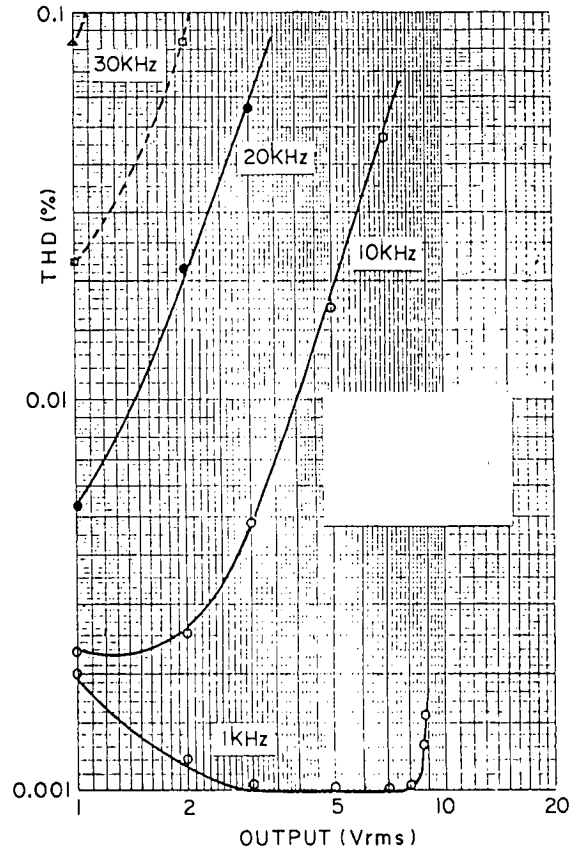

Fig. 12. Total harmonic distortion versus output voltage for operational amplifier RC 4558 without FFPS. Load 10 kΩ.
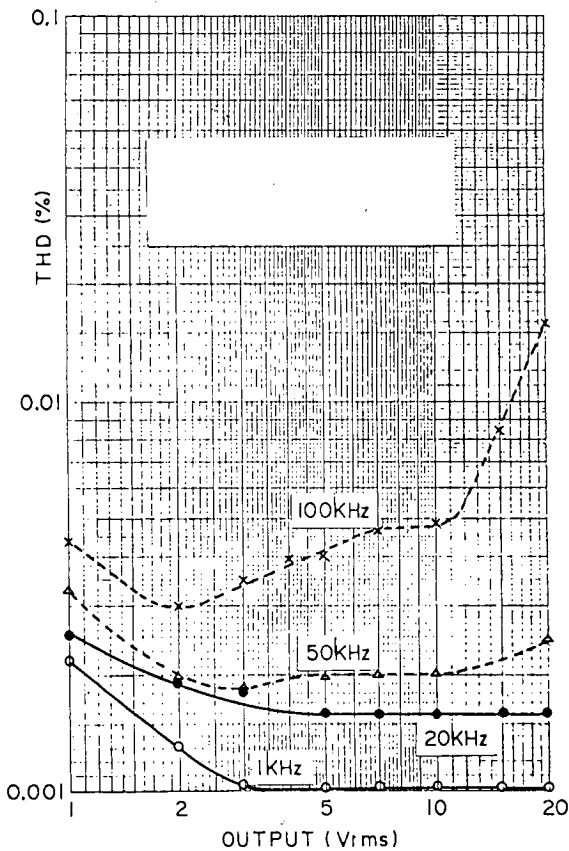

Fig. 11. Total harmonic distortion versus output voltage for operational amplifier RC 4558 with FFPS ($\pm V_{cc} = \pm 50$ V). Load 10 k Ω.
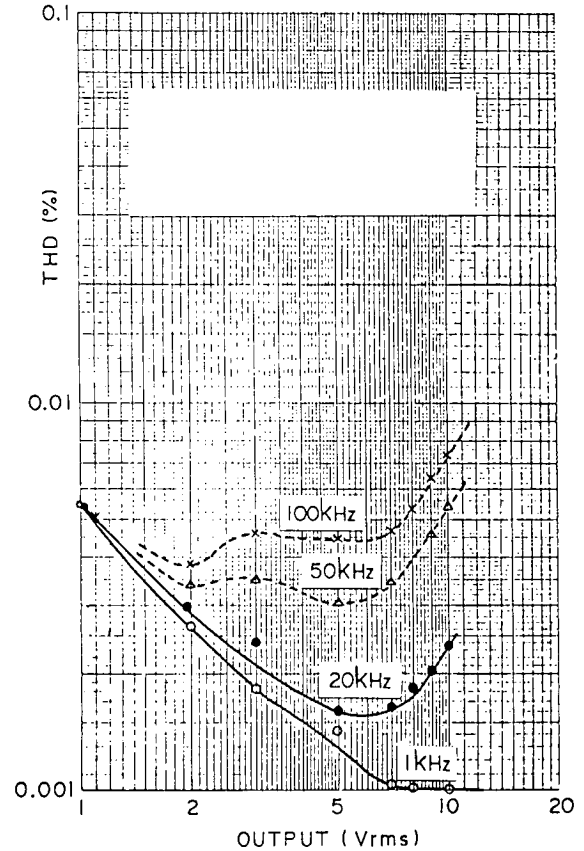

Fig. 13. Total harmonic distortion versus output voltage for FET-input operational amplifier TL-071 with FFPS. Load 10 kΩ; R_s 1–10 kΩ.
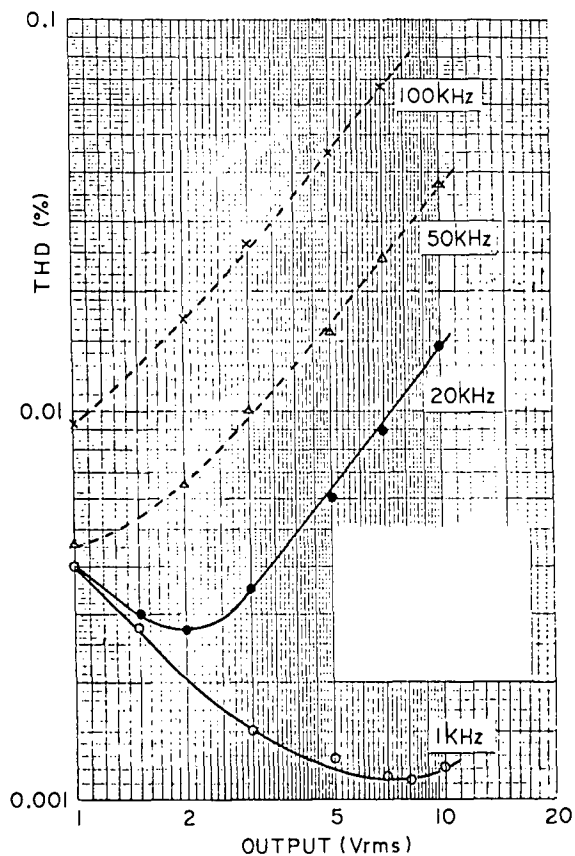
Fig. 14. Total harmonic distortion versus output voltage for FET-input operational amplifier TL-071 without FFPS. Load 10 kΩ; R_s 1 kΩ.
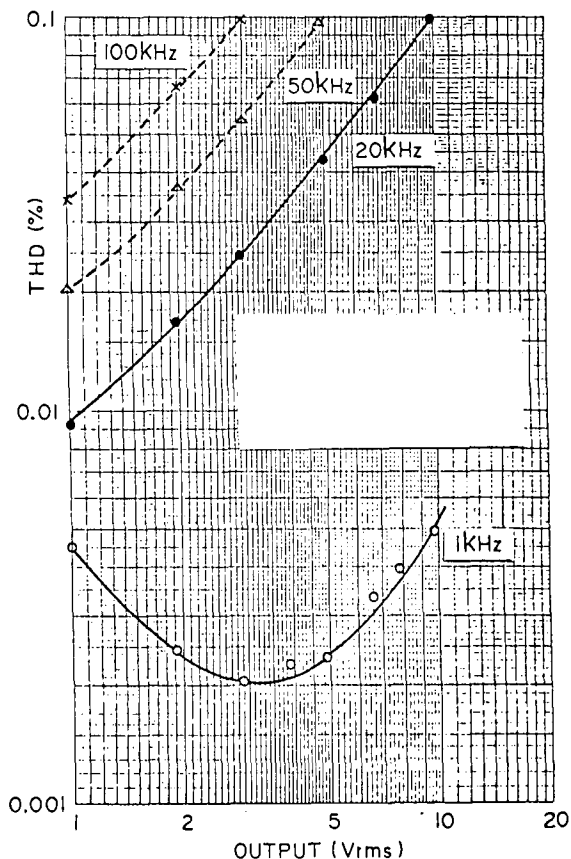
Fig. 15. Total harmonic distortion versus output voltage for FET-input operational amplifier TL-071 without FFPS. Load 10 kΩ; R_s 10 kΩ.

5.1 Active Filter with FFPS

Fig. 16 shows the circuit diagram of a high-pass filter. Active elements in filters generally result in lower signal-to-noise ratios than those for passive filters. But if the power supply voltage is set far above the rated supply voltage for the operational amplifier, the FFPS permits a signal voltage higher than the rated maximum (for example, 5 V rms without FFPS, 50 V rms with FFPS). The reference signal voltage can then be set at any desired level, preserving the required signal-to-noise ratio.

5.2 Wide-bandwidth RIAA Phonograph Preamplifier with FFPS

Fig. 17 shows the circuit diagram of an RIAA phonograph preamplifier. Noninverting preamplifiers present a unity-gain characteristic above approximately 100 kHz over a wide frequency range. The FFPS works most effectively here for a greatly improved high-frequency response.

Fig. 18 shows the total harmonic distortion characteristics of the circuit. The slew rate has increased from ±20 V/μs without FFPS to as high as ±400 V/μs with FFPS. (Since the bandwidth of the preamplifier is closely correlated with the slew rate, the bandwidth data are not presented.)

6 CONCLUSIONS

The FFPS using feedforward and boot-strap techniques is an extremely useful means for improving high-frequency response and reducing nonlinear distortion in noninverting unity-gain amplifiers. The power supply is easily designed with transistors for effective application to a circuit, which may consist of operational-amplifier integrated circuits or discrete components. The power supply is expected to find use in many applications, such as active filters, wideband phonograph preamplifiers, high-speed low-distortion buffers, and simulated inductor circuits.
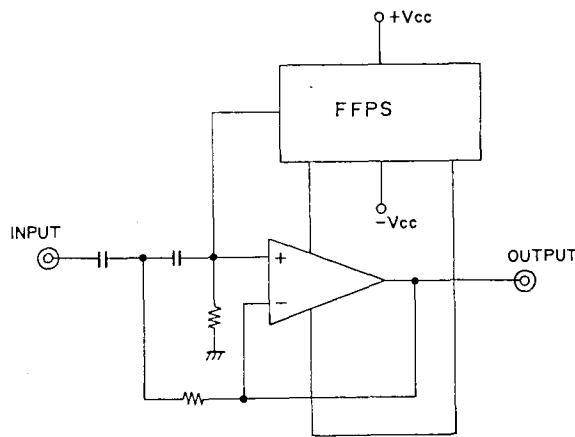
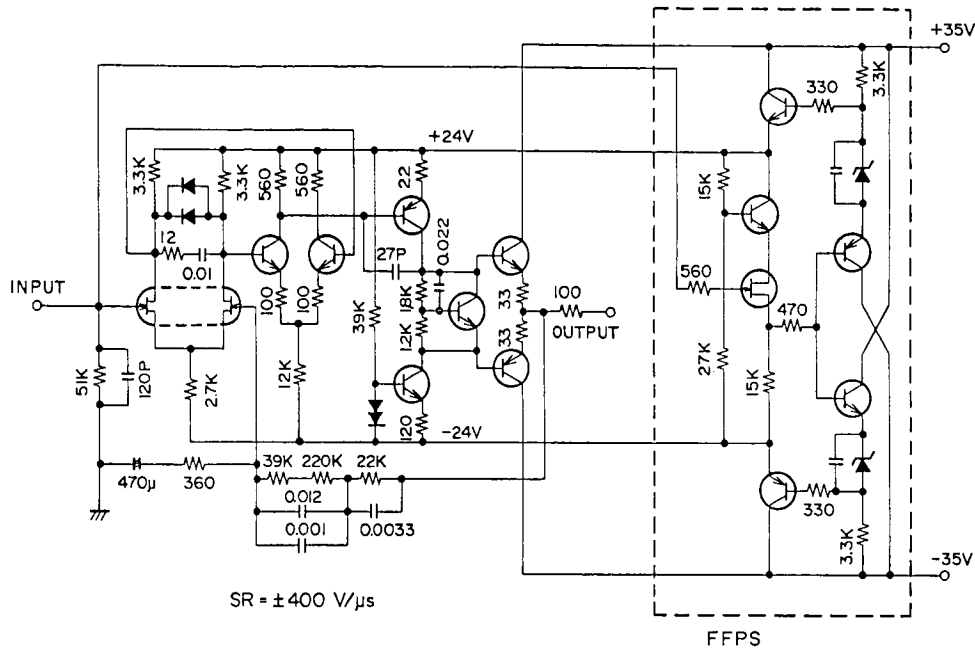Fig. 16. High-pass filter circuit with FFPS.

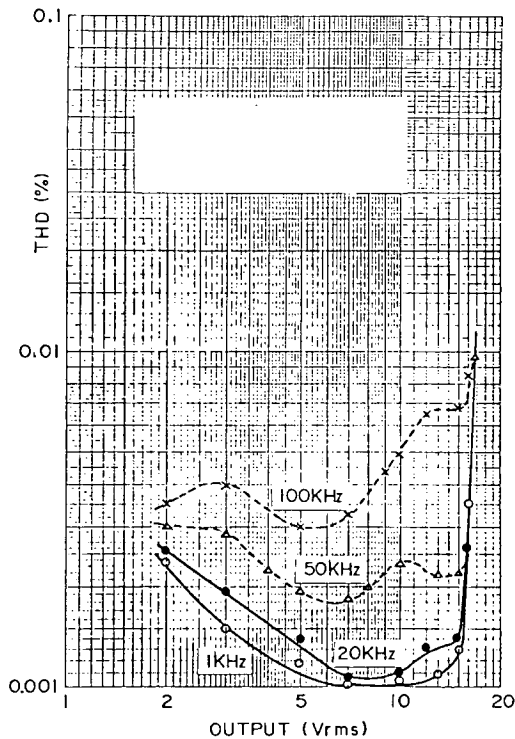Fig. 17. Wide-bandwidth RIAA phonograph preamplifier with FFPS.

Fig. 18. Total harmonic distortion versus output voltage for RIAA phonograph preamplifier of Fig. 17 with FFPS.

7 ACKNOWLEDGMENT

The authors wish to thank Mr. Hirotada Sasaki, manager of Engineering Department 1, Stereo Division, Victor Company of Japan, Ltd., and Mr. Hiroaki Suzuki of the Audio Research Center of the company for their helpful advice.

8 REFERENCES

[1] R. C. Cabot, "Measurement of Audio Signal Slew Rate," presented at the 61st Convention of the Audio Engineering Society, J. Audio Eng. Soc. (Abstracts), vol. 26, p. 988 (1978 Dec.), preprint no. 1414.

[2] J. Lammasniemi and K. Nieminen, "Distribution of the Phonograph Signal Rate of Change," presented at the 62nd Convention of the Audio Engineering Society, J. Audio Eng. Soc. (Abstracts), vol. 27, p. 424 (1979 May), preprint no. 1448.

[3] T. Holman, "New Factors in Phonograph Preamplifier Design," presented at the 52nd Convention of the Audio Engineering Society, J. Audio Eng. Soc. (Abstracts), vol. 23, p. 827 (1975 Dec.), preprint no. 1058.

[4] W. G. Jung, "Slewing Induced Distortion," Hi-Fi News & Record Rev. (1977 Nov.).

[5] W. M. Leach, "Construct a Wide Bandwidth Preamplifier," Audio (1977 Feb.).

THE AUTHORS

Eiichi Funasaka was born in Tokyo, Japan, in 1936. He graduated from Electronics Communications University in 1961 with a B.S. degree in electrical engineering. He then joined Victor Company of Japan, Ltd. (JVC) where he worked on the design and development of turntables, audio circuits, and of the CD-4 discrete 4-channel system. He is assistant general manager of the Stereo Engineering Department and is currently responsible for the development of VHD/AHD system.

Hikaru Kondou was born in Okayama, Japan, in 1948. In 1972, he received a B.S. degree in electrical engineering from Kyoto University. That year, he joined the Stereo Division of Victor Company of Japan, Ltd. (JVC), where he has been working as an engineer on the development of new circuits. In 1978, Mr. Kondou developed a new amplifier circuit called the "Super-A." He is currently responsible for the development of a new audio signal amplification technique.